

Published in final edited form as:

Cell. 2010 July 23; 142(2): 296–308. doi:10.1016/j.cell.2010.06.003.

Insulin signaling in osteoblasts integrates bone remodeling and energy metabolism

Mathieu Ferron^{1,5}, Jianwen Wei^{1,5}, Tatsuya Yoshizawa^{1,5}, Andrea Del Fattore², Ronald A. DePinho³, Anna Teti², Patricia Ducy⁴, and Gerard Karsenty^{1,*}

¹ Department of Genetics & Development, College of Physicians and Surgeons, Columbia University, New York, NY 10032, USA

² Department of Experimental Medicine, University of L'Aquila, L'Aquila, Italy

³ Department of Medicine and Genetics, Harvard Medical School, Boston, MA 02115, USA

⁴ Department of Pathology and Cell Biology, College of Physicians and Surgeons, Columbia University, New York, NY 10032, USA

Abstract

The broad expression of the insulin receptor suggests that the spectrum of insulin function has not been fully described. A cell type expressing this receptor is the osteoblast, a bone-specific cell favoring glucose metabolism through a hormone, osteocalcin, that becomes active once uncarboxylated. We show here that insulin signaling in osteoblasts is necessary for whole-body glucose homeostasis because it increases osteocalcin activity. To achieve this function insulin signaling in osteoblasts takes advantage of the regulation of osteoclastic bone resorption exerted by osteoblasts. Indeed, since bone resorption occurs at a pH acid enough to decarboxylate proteins, osteoclasts determine the carboxylation status and function of osteocalcin. Accordingly, increasing or decreasing insulin signaling in osteoblasts promotes or hampers glucose metabolism in a bone resorption-dependent manner in mice and humans. Hence, in a feed-forward loop, insulin signals in osteoblasts to activate a hormone, osteocalcin, that promotes glucose metabolism.

INTRODUCTION

Bone is a multitask tissue with mechanical, hematopoietic and metabolic functions that result from the tight interplay between two bone-specific cell types, the osteoblast and the osteoclast. Bone also emerged recently as an endocrine organ regulating glucose metabolism (Fukumoto and Martin, 2009), a function that has been ascribed to date only to the osteoblast. The intricacy existing between osteoblasts and osteoclasts raises the prospect, however, that the osteoclast may contribute to the endocrine role of the skeleton. This potential aspect of skeletal biology has never been studied.

Bone uses the osteoblast-specific secreted molecule osteocalcin to favor glucose homeostasis. Circulating osteocalcin exists in two forms, carboxylated on 3 glutamate

*Contact: gk2172@columbia.edu; Tel: (212) 305 4011; Fax: (212) 923 2090.

⁵These authors contributed equally and were placed in alphabetical order

Publisher's Disclaimer: This is a PDF file of an unedited manuscript that has been accepted for publication. As a service to our customers we are providing this early version of the manuscript. The manuscript will undergo copyediting, typesetting, and review of the resulting proof before it is published in its final citable form. Please note that during the production process errors may be discovered which could affect the content, and all legal disclaimers that apply to the journal pertain.

residues or undercarboxylated; the latter form being able to enhance insulin secretion by β -cells, insulin sensitivity and energy expenditure (Lee et al., 2007). *Osteocalcin* (*Ocn*), however, is not the only gene expressed in osteoblasts affecting glucose homeostasis. *Esp*, a gene encoding an intracellular tyrosine phosphatase called OST-PTP exerts, through its osteoblast expression, metabolic functions opposite to those of osteocalcin (Lee et al., 2007). Genetic and biochemical evidence show that *Esp* acts upstream of *Ocn* to inhibit its metabolic function. For instance, the metabolic phenotype of *Esp*^{-/-} mice is fully corrected by removing one allele of *Ocn* even though *Ocn*^{+/-} mice have no metabolic phenotype, and the fraction of undercarboxylated osteocalcin is significantly higher in *Esp*^{-/-} than in wildtype (WT) mouse serum.

The role of the osteoblast in regulating glucose metabolism revealed by these and other findings (Rached et al., 2010a; Yoshizawa et al., 2009) raises novel questions. The first one is to explain how OST-PTP, an intracellular tyrosine phosphatase, can influence the carboxylation and function of a secreted molecule like osteocalcin. A second issue is to provide evidence that the same bone-dependent regulation of glucose metabolism exists in humans since *ESP* is a pseudogene in this species (Cousin et al., 2004). A third question of physiological nature looming beyond these observations is whether insulin, in a feedback loop, influences osteocalcin synthesis and/or activity. To date none of these questions has been addressed experimentally.

The insulin receptor is a tyrosine kinase whose activity must be tightly regulated since it can be activated in the absence of ligand (Kasuga et al., 1983). Receptor tyrosine kinases are often inhibited by protein tyrosine phosphatases (PTPs) (Schlessinger, 2000) and PTP1B, which dephosphorylates the insulin receptor, is a major regulator of insulin signaling in hepatocytes and myocytes (Delibegovic et al., 2007; Delibegovic et al., 2009). The fact that OST-PTP is a tyrosine phosphatase raises the testable hypothesis that the insulin receptor is one of its substrates.

Our understanding of insulin signaling in various tissues has been profoundly altered by the analysis of mutant mouse strains lacking the insulin receptor in only one cell type (Bluher et al., 2002; Bruning et al., 1998; Konner et al., 2007; Kulkarni et al., 1999; Michael et al., 2000). Surprisingly, these studies failed to demonstrate a major influence of insulin signaling in the control of whole-body glucose homeostasis in two classical insulin target tissues, muscle and white fat (Bluher et al., 2002; Bruning et al., 1998). An implication of these observations is that insulin may act in additional organs in order to maintain glucose homeostasis. This hypothesis is consistent with the fact that the insulin receptor is expressed in many cell types where its functions have not yet been analyzed. This is particularly relevant to the osteoblast since it expresses the insulin receptor and regulates insulin secretion (Figure 1A) (Lee et al., 2007).

Here we show that the insulin receptor is a substrate of OST-PTP and PTP1B in mouse and human osteoblasts, respectively. As a result, insulin signaling in osteoblasts enhances osteocalcin activity and impacts glucose homeostasis by promoting the ability of osteoblasts to enhance bone resorption. Indeed, because the acid pH in the resorption lacuna allows protein decarboxylation it is ultimately the activity of the osteoclast that determines the carboxylation status and function of osteocalcin secreted by the osteoblast. These results reveal a novel, pH-dependent, mechanism of activation for a hormone and identify insulin signaling in osteoblasts as a critical link between bone remodeling and energy metabolism.

RESULTS

The insulin receptor is a substrate of OST-PTP in mouse osteoblasts

In order to define the mechanism whereby *Esp* affects osteocalcin carboxylation we asked whether osteocalcin and/or enzymes required for its carboxylation, γ -carboxylase and *Vkorc1* (Sadler, 2004), are phosphorylated on tyrosine residues and could be substrates of OST-PTP. We failed to detect tyrosine phosphorylation of these enzymes or of an osteocalcin peptide including all tyrosine residues of this molecule (Figure S1A–C). We also failed to detect physical interactions between osteocalcin, γ -carboxylase or *Vkorc1* and OST-PTP (Figure S1D–F). Although these negative results must be interpreted cautiously, they imply that OST-PTP does not affect osteocalcin carboxylation by acting directly on osteocalcin, γ -carboxylase or *Vkorc1*.

To pursue our search we used substrate trapping, an assay using phosphatase domains in which a single amino acid substitution abrogates their catalytic activity, not their ability to recognize substrates (Flint et al., 1997).

We used OST-PTP active phosphatase domain (Chengalvala et al., 2001) to test whether the insulin receptor (InsR) was a substrate of OST-PTP for the following reasons. First, dephosphorylation of the InsR by another tyrosine phosphatase, PTP1B, regulates insulin signaling in other cell types (Delibegovic et al., 2007; Delibegovic et al., 2009). Second, OST-PTP has homology in its catalytic domain to phosphatases dephosphorylating the InsR (Figure S1G). Third, the InsR is abundant in osteoblasts and treatment of osteoblasts with insulin increases phosphorylation of the InsR and its downstream targets AKT, GSK3 β , FoxO1 and p70S6K (Figures 1A and S1H). Fourth, InsR phosphorylation increased in bone in a time-dependent manner following insulin injection in vivo (Figure 1B). Furthermore, we reasoned that if osteoblasts favor glucose homeostasis insulin signaling should influence osteoblast biology.

The InsR interacted with a mutated form of OST-PTP or of PTP1B, a positive control, but not with negative controls such as wildtype (WT) OST-PTP, PTP1B or glutathione S-transferase (GST); InsR interaction with OST-PTP was competed by increasing concentrations of orthovanadate, OST-PTP interacted with InsR in cells following insulin treatment only, and did not interact with an unrelated tyrosine kinase receptor (Figure 1C–E). Furthermore, WT OST-PTP dephosphorylated in vitro InsR while a mutant form of OST-PTP lacking its phosphatase activity did not (Figures 1E and 1F). Consistent with these results, phosphorylation of InsR on tyrosines 1150 and 1151 and of FoxO1, a target of insulin signaling (Puigserver et al., 2003), was increased in *Esp*^{−/−} osteoblasts (Figures 1G, S1I and S1J). These experiments provide congruent biochemical evidence indicating that InsR is a substrate of OST-PTP in mouse osteoblasts.

Insulin signaling in osteoblasts is a determinant of whole body glucose metabolism

That insulin signaling in osteoblasts is regulated by OST-PTP, a phosphatase affecting glucose metabolism, implies that it also influences this process. To address this question, we generated osteoblast-specific *Insulin Receptor (InsR)*-deficient mice (*InsR_{osb}*^{−/−} mice) by crossing *al(I)collagen-Cre* transgenic mice, which delete genes in osteoblasts only (Dacquin et al., 2002), with mice harboring a floxed allele of *InsR* (Figures S2A–C). Western blot analysis of osteoblasts showed at least 60% deletion of the InsR in osteoblasts but not in liver, pancreas, white adipose tissue, muscle and brain of *InsR_{osb}*^{−/−} mice (Figures S2D–F).

InsR_{osb}^{−/−} mice were born at the expected Mendelian ratio and presented at 8 weeks of age a significant elevation of blood glucose in the fed state and a significant reduction of serum

insulin levels in the fasted or fed state, glucagon levels being unaffected (Figures 2A, 2B and S2G). A glucose stimulated insulin secretion (GSIS) test verified that insulin secretion was decreased in *InsR_{osb}^{-/-}* mice (Figure 2C). There was also a decrease in the number of islets, islet size, β -cell mass, β -cell proliferation and insulin content in *InsR_{osb}^{-/-}* compared to control pancreata (Figure 2D). As a result of this decrease in insulin secretion a glucose tolerance test (GTT) demonstrated glucose intolerance in *InsR_{osb}^{-/-}* mice (Figures 2E and S2H). Insulin tolerance, as measured by an insulin tolerance test (ITT), was also significantly reduced in *InsR_{osb}^{-/-}* compared to control mice (Figures 2F and S2I). Hence, analysis of *InsR_{osb}^{-/-}* mice revealed that insulin signaling in osteoblasts contributes to whole-body glucose homeostasis by increasing β -cell proliferation and insulin secretion and energy expenditure (Figures 2H, S2J and S2K).

Insulin often transmits its signal by inhibiting FoxO1 activity. Since FoxO1 affects glucose homeostasis through its expression in osteoblasts (Rached et al., 2010a) we asked whether it was downstream of the insulin signaling pathway in these cells by generating *InsR_{osb}^{-/-}* mice lacking one copy of *FoxO1* only in osteoblasts (*InsR_{osb}^{-/-};FoxO1_{osb}^{+/-}* mice). As expected if *FoxO1* does lie downstream of insulin signaling in osteoblasts, decreasing its expression corrected the glucose intolerance of *InsR_{osb}^{-/-}* mice. This result indicates that inhibiting FoxO1 is a mean whereby insulin signaling in osteoblasts affects glucose homeostasis (Figure 2I–L).

Insulin signaling in osteoblasts acts upstream of *Osteocalcin*

Since OST-PTP inhibits osteocalcin activity, the observation that InsR is its substrate implies that insulin signaling in osteoblasts and osteocalcin lie in the same metabolic pathway.

To test this hypothesis we first generated mice lacking one allele of *Osteocalcin* and one allele of *InsR* in osteoblasts (*Ocn^{+/-};InsR_{osb}^{+/-}* mice) hypothesizing that, if the 2 genes lie in the same pathway these compound heterozygous mutant mice should display a phenotype reminiscent of the one observed in *Ocn^{-/-}* mice. Indeed, whether we studied glucose in fed state, insulin secretion, glucose or insulin tolerance *Ocn^{+/-};InsR_{osb}^{+/-}* mice had metabolic abnormalities similar to the ones of *Ocn^{-/-}* mice (Figure 3A–E), *InsR_{osb}^{+/-}* and *Ocn^{+/-}* mice were undistinguishable from control littermates. Likewise, if OST-PTP inhibits the function of insulin signaling in osteoblasts one would anticipate that the metabolic phenotype of *Esp^{-/-}* mice should be corrected by decreasing insulin signaling in osteoblasts. Accordingly, removing one allele of *InsR* in osteoblasts from *Esp^{-/-}* mice normalized glucose and insulin tolerance (Figure 3F–H). These two experiments provide genetic evidence that a function of insulin signaling in osteoblasts is to favor osteocalcin metabolic activity (Figure 3I).

That reducing insulin signaling in osteoblasts corrected the enhanced glucose and insulin tolerance of *Esp^{-/-}* mice was important in its own right as it indicated that the metabolic phenotype of *Esp^{-/-}* mice is secondary to an increase in insulin signaling in osteoblasts. This contention is supported by the increased phosphorylation of the InsR in *Esp^{-/-}* osteoblasts (Figure 1H). Thus in subsequent experiments studying insulin signaling in osteoblasts we relied on both loss- (*InsR_{osb}^{-/-}*) and gain-of-function (*Esp^{-/-}*) models.

Insulin signaling in osteoblasts inhibits osteocalcin carboxylation

To ascertain that insulin signaling in osteoblasts regulates osteocalcin activity we developed a dual ELISA quantifying the ratio between undercarboxylated, i.e. active (GLU), and carboxylated, i.e. inactive (GLA), circulating osteocalcin (Figure S3A–E).

This ELISA detected an increase in undercarboxylated osteocalcin in *Esp*^{-/-} mice, which harbor an increase in insulin signaling in osteoblasts (Figure 3H) but not in *Esp*^{-/-}; *InsR_{osb}*^{+/-} mice that do not (Figure 3J). In contrast, it showed that undercarboxylated osteocalcin levels were decreased when insulin signaling is impaired in osteoblasts (*InsR_{osb}*^{-/-} mice), even though *Ocn* expression and serum levels were not affected (Figures 3J, S3F and S3G). A decrease in undercarboxylated osteocalcin was also observed in *Ocn*^{+/-}; *InsR_{osb}*^{+/-} mice that display a glucose intolerance similar to the one of the *Ocn*^{-/-} and *InsR_{osb}*^{-/-} mice (Figures 3J and S6H). These measurements of undercarboxylated osteocalcin in various mutant mouse strains along with the genetic evidence presented above indicate that insulin signaling in osteoblasts inhibits osteocalcin carboxylation, i.e. is a positive regulator of its metabolic activity.

Insulin signaling in osteoblasts favors bone resorption

In a separate line of work we noticed in *InsR_{osb}*^{-/-} mice a marked decrease in the serum level of CTx a marker of bone resorption, while this parameter was increased in *Esp*^{-/-} mice (Figure 4A). This data suggested that insulin signaling in osteoblasts favors bone resorption. Although not the focus of this study bone formation parameters were severely decreased in *InsR_{osb}*^{-/-} mice; as a result these mice had a low bone mass (Figure S4A).

To prove that insulin signaling in osteoblasts affects bone resorption we used a co-culture assay of osteoblasts and osteoclasts (Takahashi et al., 1988). When co-cultured with WT osteoblasts, WT osteoclast precursor cells differentiated and formed resorption pits. When WT osteoclast precursor cells were co-cultured with *InsR*^{-/-} osteoblasts the area covered by resorption pits was significantly decreased while it was increased 50% when they were co-cultured with *Esp*^{-/-} osteoblasts (Figure 4B). That the number of osteoclasts was unaffected whether we used *Esp*^{-/-} or *InsR*^{-/-} osteoblasts (Figure 4B) is consistent with the notion that insulin signaling in osteoblasts promotes only the function of osteoclasts.

We next studied expression, in osteoblasts, of genes influencing bone resorption and noticed that expression of *Osteoprotegerin* (*Opg*), a gene encoding a decoy receptor for RANKL and a negative regulator of osteoclast function (Teitelbaum and Ross, 2003), was increased 2-fold in *InsR*^{-/-} and decreased 50% in *Esp*^{-/-} osteoblasts; its secretion followed the same pattern (Figure 4C–E). That insulin treatment of WT but not of *InsR*^{-/-} osteoblasts decreased *Opg* expression and secretion verified that it is an insulin target gene in osteoblasts (Figure 4E). To demonstrate that a moderate increase in OPG secretion promotes the activity rather than the differentiation of osteoclasts we cultured osteoclast progenitor cells in the presence of increasing amount of OPG (0 to 90ng/ml). Low amounts of OPG in the culture medium decreased the surface covered by resorption pits but not the osteoclasts number (Figure 4F).

Multiple evidences indicated that insulin signaling in osteoblasts favors bone resorption by inhibiting FoxO1. First, *Opg* expression was increased 2-fold in ROS17/2.8 osteoblastic cells overexpressing FoxO1 (Figure 4G). Second, siRNA-mediated downregulation of FoxO1 decreased *Opg* expression and secretion in mouse osteoblasts (Figures 4H and S4B). Third, the increase in bone resorption noted in *FoxO1_{obs}*^{-/-} mice (Rached et al., 2010b) could be traced to a decrease in *Opg* expression in bone (Figure 4I). Fourth, removing one allele of *FoxO1*, in osteoblasts only, from *InsR_{osb}*^{-/-} mice normalized bone resorption (Figure 4J).

Insulin signaling in osteoblasts promotes the osteoclasts ability to acidify the bone extracellular matrix (ECM)

Next we sought to identify *Opg*-dependent molecular events taking place in osteoclasts under the control of insulin signaling in osteoblasts. Expression of *CathepsinK* (*Ctsk*) and *Tcirg1*, two genes implicated in bone resorption, was decreased in *InsR_{osb}^{-/-}* and increased in *Esp^{-/-}* bones (Figure 4K). *Ctsk* and *Tcirg1* expression was also decreased in osteoclasts obtained following co-culture of WT osteoclast precursor cells with *InsR^{-/-}* osteoblasts (Figure 4L). For the rest of this study we focused on *Tcirg1*, a gene encoding a vacuolar proton pump subunit essential for acidification of the bone ECM, precisely because acidification of the bone ECM is a pre-requisite for bone resorption (Teitelbaum and Ross, 2003).

Taken together, the biochemical, molecular and genetic evidences presented above indicate that insulin signaling in osteoblasts decreases *Opg* expression and the *Opg*/*Rankl* ratio (Figure 4M); this results in an increase in *Tcirg1* expression, in ECM acidification and in bone resorption.

Bone resorption as a means to decarboxylate osteocalcin

An acid pH can decarboxylate proteins (Engelke et al., 1991); this raised the prospect that bone resorption, that occurs at an acid pH, could be a mechanism decarboxylating osteocalcin in vivo.

To verify that an acid pH could decarboxylate and activate osteocalcin, equal amounts of carboxylated osteocalcin were incubated for 2 weeks at 37°C in solutions buffered at either pH 7.5 or pH 4.5, the latter being the pH present in the resorption lacunae (Silver et al., 1988). Each osteocalcin solution was then analyzed by high-resolution mass spectrometry. This revealed a peak at m/z 1325.103⁽⁺⁴⁾ corresponding to a form of osteocalcin in which all three glutamic residues are carboxylated (molecular weight: 5296.42 Da) and another peak at m/z 1314.108⁽⁺⁴⁾ corresponding to an osteocalcin form in which one of the three glutamic residues was not carboxylated (molecular weight: 5252.43 Da) (Figure 5A). The mass difference between these two forms is 43.9 Da, which corresponds to one carboxylation modification.

Importantly, the ratio of undercarboxylated to fully carboxylated osteocalcin was significantly increased when osteocalcin was incubated at pH 4.5 (Figure 5A). Tandem mass spectrometry analysis of trypsin-digested samples demonstrated that the presence of a GLU residue at position 13 was increased more than 2-fold upon incubation at pH 4.5 (Figure 5B), thus suggesting that this residue is highly susceptible to decarboxylation. We also assessed the metabolic activity of these two preparations of osteocalcin. When rat insulinoma INS-1 cells were treated with carboxylated (pH 7.5) or undercarboxylated (pH 4.5) osteocalcin, only the latter form could increase insulin secretion to the same extent as recombinant uncarboxylated osteocalcin used as positive control (Ferron et al., 2008) (Figure 5C).

Given these results we cultured osteoclast precursor cells in the presence or absence of RANKL on bovine cortical bone slides devitalized to exclude any endogenous osteoblastic activity. Two days after osteoclasts were identifiable total, carboxylated and undercarboxylated osteocalcin were measured. When osteoclast differentiation had been triggered by RANKL, the levels of total and undercarboxylated (GLU) osteocalcin were increased while the one of carboxylated (GLA) osteocalcin was decreased; as a result there was a 2-fold increase in the GLU/GLA ratio (Figures 5D and 5E). Thus, the resorptive activity of osteoclasts suffices to activate osteocalcin.

The osteoclast ability to acidify the bone ECM favors glucose homeostasis

Given the role of osteocalcin in glucose metabolism we next asked whether the osteoclasts ability to activate osteocalcin affects glucose metabolism.

For that purpose we analyzed *oc/oc* harboring a loss-of-function mutation in *Tcirg1* resulting in osteopetrosis (Scimeca et al., 2000). Level of undercarboxylated osteocalcin was decreased 30% in *oc/oc* compared to WT serum (Figure 5F). Accordingly, conditioned medium of *oc/oc* calvaria cultures did not stimulate insulin secretion by INS-1 cells (Figure 5G). Hence, in *oc/oc* mice whose osteoclasts cannot acidify the bone ECM, circulating osteocalcin is metabolically inactive.

Importantly for our purpose *oc/oc* mice were also glucose intolerant (Figures 5H and 5I) with a marked decrease in serum insulin levels, pancreas insulin content and *Insulin* expression in pancreas (Figure 5J–L). To determine whether this phenotype was secondary to a function of *Tcirg1* in osteoclasts, we transplanted *oc/oc* fetal liver hematopoietic stem cells into WT irradiated mice. Transplantation of mutant hematopoietic stem cells resulted in high bone mass in WT recipient animals since their osteoclasts could not form resorption pits (Figures 5M and S5B–F). Fasting glucose blood levels were increased while serum insulin levels in fasted and fed states were decreased in mice transplanted with *oc/oc* cells (Figures 5N and 5O). A GSIS test demonstrated a defect in insulin secretion in these mice, while a GTT showed glucose intolerance (Figure 5P–R). Energy expenditure was also decreased in WT mice transplanted with *oc/oc* cells (Figures 5S and S5G–H). As expected, there was in mice transplanted with *oc/oc* cells a significant decrease in serum undercarboxylated osteocalcin while the total osteocalcin level was unchanged (Figures 5T and S6G). These results demonstrate that the osteoclasts ability to acidify the bone ECM is both necessary and sufficient to activate osteocalcin and to influence whole-body glucose metabolism.

Insulin signaling in osteoblasts favors glucose homeostasis in a bone resorption-dependent manner

The observations presented above beg the following question: is it because it favors bone resorption that insulin signaling in osteoblasts promotes glucose homeostasis?

To determine whether the influence of insulin signaling in osteoblasts on glucose metabolism depends on the osteoclasts ability to acidify the bone ECM we generated mice lacking one allele of *InsR* in osteoblasts and harboring one *oc* allele (*InsR_{osb}^{+/-};oc/+* mice). In these mutant mice osteocalcin undercarboxylation was markedly decreased (Figure 6A); as a result of this shift toward decreased osteocalcin activity, insulin secretion, glucose and insulin tolerance were impaired in *InsR_{osb}^{+/-};oc/+* but not in *InsR_{osb}^{+/-}* or *oc/+* mice (Figures 6B–D and S6A). These data link genetically insulin signaling in osteoblasts, bone resorption and whole body glucose homeostasis.

If insulin signaling in osteoblasts promotes glucose homeostasis in a bone resorption-dependent manner then inhibiting bone resorption in a model of increased insulin signaling in osteoblasts such as the *Esp*^{-/-} mice should correct their metabolic phenotypes. Indeed and unlike *Esp*^{-/-} mice, *Esp*^{-/-};oc/+ mice had normal bone resorption, normal osteocalcin carboxylation status (Figures 6E and 6F), normal insulin secretion, normal glucose and insulin tolerance (Figures 6G–I and S6B). Likewise when we treated *Esp*^{-/-} mice with alendronate, an inhibitor of osteoclast activity (Fisher et al., 1999), osteocalcin carboxylation, insulin secretion, glucose and insulin tolerance were normalized (Figures 6J–N and S6C).

Lastly, if insulin signaling in osteoblasts promotes glucose metabolism by increasing bone resorption, stimulating bone resorption should rescue, at least partially, glucose intolerance in WT mice. To test this contention we fed WT mice a high fat diet and treated them with RANKL or GST as a negative control. As expected, RANKL increased bone resorption parameters (Figures S6D and S6E). This increase in bone resorption led to a 3-fold increase in serum levels of undercarboxylated osteocalcin (Figure 6O). RANKL-treated mice fed a high fat diet secreted more insulin, were significantly less glucose intolerant, more insulin tolerant and less fat than GST-treated mice (Figures 6P–S and S6F). These three experiments demonstrate that insulin signaling in osteoblasts cannot affect osteocalcin activity and glucose metabolism if bone resorption is impaired.

Insulin signaling in human osteoblasts, bone resorption, osteocalcin activity and glucose homeostasis

Clinical studies indicate that osteocalcin is involved in glucose homeostasis in humans (Hwang et al., 2009; Kanazawa et al., 2009; Pittas et al., 2009). However, since *ESP* is a pseudogene in humans (Cousin et al., 2004) osteocalcin activity must be regulated by another phosphatase. The identification of InsR as a substrate of OST-PTP provided a way to address this question.

We asked whether PTP1B, a tyrosine phosphatase able to dephosphorylate INSR, was present in human osteoblasts. PTP1B was markedly more abundant in human than in mouse osteoblasts and decreasing its expression in human osteoblasts increased INSR and FOXO1 phosphorylation and decreased *OPG* expression (Figures 7A–D). Conversely, siRNA-mediated knockdown of INSR in human osteoblasts decreased FOXO1 phosphorylation and increased *OPG* expression (Figures 7D and 7E). Finally, PTP1B could trap INSR in human osteoblasts (Figure 7F). Thus insulin signaling in human osteoblasts is regulated by a tyrosine phosphatase and favors bone resorption.

The observations made in mice imply that patients harboring a defect in bone resorption (osteopetrosis) should have low serum undercarboxylated osteocalcin and serum insulin levels. We tested this contention by analyzing patients with an autosomal dominant form of osteopetrosis. Three patients had a missense mutation in *CICN7*, a gene required for acid secretion in the resorption lacuna (Schaller et al., 2005); for the others, although no genetic defect could be identified, a decrease of acidification ability was demonstrated in osteoclasts cultured *ex vivo* in presence of LysoSensor fluorescent pH indicators (Figures S7A and S7B). Circulating undercarboxylated osteocalcin was significantly decreased in all patients, as were serum insulin levels measured after feeding (Figure 7G). These data support the notion that osteocalcin activity is determined in humans, in part, by bone resorption, an aspect of bone remodeling regulated by insulin signaling in osteoblasts.

Discussion

This study demonstrates that insulin signaling in osteoblasts is a significant determinant of whole-body glucose homeostasis. Taking full advantage of the interplay between osteoblasts and osteoclasts characterizing bone remodeling, insulin signaling in osteoblasts achieves this function by favoring osteocalcin carboxylation (Figure 7H). Thus this study identifies insulin as a key molecular link between bone remodeling and energy metabolism.

Insulin signaling in osteoblasts and glucose homeostasis

Insulin signaling and functions in various tissues have been extensively studied *in vivo* in the last 10 years using mutant mouse strains lacking the insulin receptor in only one cell type. These studies have redefined the respective contributions of various cell types to

whole-body glucose homeostasis. For instance, they showed that insulin signaling in β -cells is needed for insulin secretion and, as expected, insulin signaling in hepatocytes is needed for insulin sensitivity (Kulkarni et al., 1999; Michael et al., 2000). In contrast, deletion of this receptor in white adipose tissue (WAT) resulted in an improvement of glucose metabolism (Bluher et al., 2002). Taken together these various studies imply that insulin exerts yet to be identified functions in other tissues, an idea congruous with the fact that the insulin receptor is expressed in many cell types where its function has not been studied yet.

In agreement with this hypothesis, we show here, through the analysis of both loss- and gain-of-function models, that insulin signaling in osteoblasts influences whole-body glucose homeostasis by promoting insulin secretion. To the best of our knowledge osteoblasts and hepatocytes are the only cell types in which disrupting insulin signaling hampers glucose metabolism in mice fed a normal diet.

Insulin signaling in osteoblasts, osteocalcin activation and bone resorption

One issue surrounding osteocalcin biology has been to elucidate how the intracellular phosphatase OST-PTP could favor its carboxylation. We identify here the insulin receptor as a bona fide substrate of OST-PTP. This finding means that the metabolic phenotype of the OST-PTP-deficient mice characterized by improved whole-body glucose homeostasis (Lee et al., 2007) is due to an increase in insulin signaling in osteoblasts.

More importantly, since OST-PTP regulates osteocalcin function these results also placed *de facto* insulin signaling in osteoblasts upstream of osteocalcin. To increase osteocalcin bioactivity insulin signaling in osteoblasts acts in a ricocheting manner using the huge amount of osteocalcin stored in the bone ECM and the interplay between osteoblasts and osteoclasts. Specifically, it takes advantage of the ability of the osteoblast to promote bone resorption. Since an acid pH is the only known chemical condition allowing protein decarboxylation (Engelke et al., 1991), bone resorption, which occurs at pH 4.5, provides an ideal setting to decarboxylate and activate osteocalcin (Figure 7H).

The positive feedback loop existing between insulin signaling in osteoblasts and osteocalcin functions implies that negative regulators of this process may also exist. Leptin, another hormone exerting a major influence on energy metabolism, is one of them and does so also by modulating *Esp* expression (Hinoi et al., 2008). Thus, these studies highlight the unexpected importance of *Esp* in orchestrating the endocrine function of bone.

Another issue about osteocalcin biology has been to provide evidence that it has the same function in humans. Several arguments indicate that it is the case. First, the tyrosine phosphatase PTP1B fulfills in human osteoblasts the function that OST-PTP fulfills in mouse osteoblasts. Second, insulin signaling in human osteoblasts regulates *OPG* expression as it does in mouse osteoblasts. Third, osteopetrotic patients and mice display the same increase in osteocalcin carboxylation and decrease in insulin blood levels. These results support a growing number of observations linking osteocalcin or warfarin, a compound decreasing its carboxylation, to the regulation of glucose homeostasis in humans (Hwang et al., 2009; Kanazawa et al., 2009; Pittas et al., 2009; Scheen, 2005). The notion that hampering bone resorption has deleterious consequences on glucose homeostasis is medically important since most drugs used to treat osteoporosis target this aspect of bone remodeling. Specifically, fasting plasma glucose levels are elevated in osteoporotic women treated with drugs inhibiting bone resorption and serum undercarboxylated osteocalcin levels are positively correlated with bone resorption in healthy women (Kaji et al., 2009; Yamauchi et al.).

Lastly, this work expands the relationship existing between bone remodeling and energy metabolism (Karsenty, 2006) and raises the testable hypothesis that the skeleton may exert additional endocrine influences on other, yet to be identified, physiological functions.

EXPERIMENTAL PROCEDURES

Mice generation

Generation of *Esp*^{-/-} (C57BL/6J;129/Sv), *Ocn*^{-/-} (C57BL/6J;129/Sv) and *FoxO1_{obs}*^{-/-} (C57BL/6J;BALB/c) mice was reported (Dacquin et al., 2004; Ducy et al., 1996; Rached et al., 2010a). *InsR_{obs}*^{-/-} mice were generated by intercrossing the progeny of crosses between *InsR^{lox/lox}* mice, that harbor LoxP sites within introns 3 and 4 (Figure S2A), and *α1(I)collagen-Cre* transgenic mice (Dacquin et al., 2002). *oc*^{+/+} mice (C57BL/6J;C3H) were obtained from The Jackson Laboratory. Genetic backgrounds of mice are as follows: *InsR_{obs}*^{-/-} (C57BL/6J:87.5%; 129/Sv:12.5%), *Ocn*^{+/-};*InsR_{obs}*^{+/-} and *Esp*^{-/-};*InsR_{obs}*^{+/-} (C57BL/6J;129/Sv), *FoxO1_{obs}*^{+/-};*InsR_{obs}*^{-/-} (C57BL/6J;BALB/c;129/Sv), *oc*^{+/+};*InsR_{obs}*^{+/-} (C57BL/6J;C3H;129/Sv). Control littermates were used in all experiments. Mice genotypes were determined by PCR; primer sequences are available upon request. CD45.2⁺ fetal liver stem cells isolated from E14.5 WT or *oc/oc* embryos were transplanted (2×10^6 /mice) via tail vein injection into 5 week-old CD45.1⁺ irradiated WT recipient mice. Hematopoietic reconstitution was quantified by FACS analysis of blood cells collected 10 weeks post-transplantation (Figure S6B–E).

Metabolic studies and bioassays

Glucose tolerance test (GTT), glucose stimulated insulin secretion (GSIS), insulin tolerance test (ITT), pancreas insulin content, histology and high fat diet studies were performed as described (Lee et al., 2007). ELISA were used to measure mouse/human insulin (Mercodia), plasma glucagon (ALPCO), mouse CTx (RatLaps, IDS), bovine/human osteocalcin carboxylation ratios (Takara), human TRAP (Bone TRAP Assay, IDS) and human CTx (Serum Crosslaps, IDS).

Biochemistry and gene expression studies

A complete description of all biochemical experiments is available as Supplemental Material and Methods. All antibodies were obtained from Cell Signaling Technology, with the exception of anti-PTP1B (R&D), anti-FLAG and anti-β-actin (Sigma). RNA isolation, cDNA preparation and real-time PCR analyses were carried out following standard protocols. Substrate-trapping was conducted as described (Flint et al., 1997). Briefly, extracts from pervanadate-treated cells were incubated in the presence of GST recombinant protein and washed 4 times with lysis buffer. For in vitro dephosphorylation assays ROS17/2.8 cells were treated with pervanadate (100 μM) for 30 min and InsR was immunoprecipitated. The immune complex was then incubated at 30°C in the presence of 1 μg of recombinant GST, GST-PTP or GST-PTPDA for indicated times. Phosphorylation of InsR was visualized by western blot. In in vivo trapping experiments, MG-63 or ROS17/2.8 cells were transfected with FLAG-tagged expression vector and complexes were immunoprecipitated using anti-FLAG antibodies.

Cell culture

Human osteoblastic cells hFOB 1.19, Saos-2 (ATCC) or mouse primary osteoblasts were transfected with siRNA pools (On-target, Dharmacon) according to the manufacturer instructions. *InsR*^{+/+} and *InsR*^{-/-} osteoblasts were generated *ex vivo* by infecting *InsR^{lox/lox}* with either GFP- or Cre-expressing adenovirus (University of Iowa). Bone marrow progenitor cells and osteoblasts co-cultures were performed as previously described

(Takahashi et al., 1988). In vitro resorption activity of osteoclasts was measured using BD BioCoat™ Osteologic™ Bone Cell Culture System.

Mass spectrometry

Synthetic carboxylated osteocalcin (Bio-Synthesis Inc.) was incubated at 37°C in pH 7.5 or pH 4.5 0.1M phosphate buffer for 2 weeks. Mass spectrometry was run using Bruker Apex 9.4T Fourier Transform Ion Cyclotron Resonance (FT-ICR) Mass Spectrometer and Daltonics DataAnalysis software (v. 3.4) for analysis. Comparative quantification between carboxylated and undercarboxylated osteocalcin were made based on exact mass measurements and fit of isotopic peaks to that of theoretical isotopic patterns (SNAP2 algorithm).

Statistics

Results are given as means ± standard errors of the mean except in human studies in which standard deviations were used. Statistical analyses were performed using unpaired, two-tailed Student's t test for comparison between two groups and One-way ANOVA test for more than two groups comparison. For GTT, ITT and GSIS, we performed Two-way mixed designed ANOVA and calculated Area Under the Curve (AUC) followed by student's t-test or One-way ANOVA. For all experiments (*p or #p) ≤ 0.05, (**p or ##p) ≤ 0.01, ***p ≤ 0.001.

Supplementary Material

Refer to Web version on PubMed Central for supplementary material.

Acknowledgments

We thank Drs S. Kousteni, T. Zee, R.L. Levine, M. Tremblay, and J. Vacher for reagents, Dr. J. Lacombe for help with transplantations, Drs K. Henriksen and J. Bollerslev for generously sharing patient serum samples, Dr. T. Lam at the W.M. Keck Foundation Biotechnology Resource Laboratory, Yale University, for FT-ICR mass spectral analyses, Drs. J.K. Kim and F. Mauvais-Jarvis for critical reading of the manuscript. This work was supported by a fellowship from the Fond de la recherche en santé du Québec (M.F.) and grants from the NIH (G.K.) and the Juvenile Diabetes Research Foundation (P.D.).

References

- Bluher M, Michael MD, Peroni OD, Ueki K, Carter N, Kahn BB, Kahn CR. Adipose tissue selective insulin receptor knockout protects against obesity and obesity-related glucose intolerance. *Dev Cell*. 2002; 3:25–38. [PubMed: 12110165]
- Bruning JC, Michael MD, Winnay JN, Hayashi T, Horsch D, Accili D, Goodyear LJ, Kahn CR. A muscle-specific insulin receptor knockout exhibits features of the metabolic syndrome of NIDDM without altering glucose tolerance. *Mol Cell*. 1998; 2:559–569. [PubMed: 9844629]
- Chengalvala MV, Bapat AR, Hurlburt WW, Kostek B, Gonder DS, Mastroeni RA, Frail DE. Biochemical characterization of osteo-testicular protein tyrosine phosphatase and its functional significance in rat primary osteoblasts. *Biochemistry*. 2001; 40:814–821. [PubMed: 11170399]
- Cousin W, Courseaux A, Ladoux A, Dani C, Peraldi P. Cloning of hOST-PTP: the only example of a protein-tyrosine-phosphatase the function of which has been lost between rodent and human. *Biochem Biophys Res Commun*. 2004; 321:259–265. [PubMed: 15358244]
- Dacquin R, Mee PJ, Kawaguchi J, Olmsted-Davis EA, Gallagher JA, Nichols J, Lee K, Karsenty G, Smith A. Knock-in of nuclear localised beta-galactosidase reveals that the tyrosine phosphatase Ptp^{prv} is specifically expressed in cells of the bone collar. *Dev Dyn*. 2004; 229:826–834. [PubMed: 15042706]

- Dacquin R, Starbuck M, Schinke T, Karsenty G. Mouse alpha1(I)-collagen promoter is the best known promoter to drive efficient Cre recombinase expression in osteoblast. *Dev Dyn.* 2002; 224:245–251. [PubMed: 12112477]
- Delibegovic M, Bence KK, Mody N, Hong EG, Ko HJ, Kim JK, Kahn BB, Neel BG. Improved glucose homeostasis in mice with muscle-specific deletion of protein-tyrosine phosphatase 1B. *Mol Cell Biol.* 2007; 27:7727–7734. [PubMed: 17724080]
- Delibegovic M, Zimmer D, Kauffman C, Rak K, Hong EG, Cho YR, Kim JK, Kahn BB, Neel BG, Bence KK. Liver-specific deletion of protein-tyrosine phosphatase 1B (PTP1B) improves metabolic syndrome and attenuates diet-induced endoplasmic reticulum stress. *Diabetes.* 2009; 58:590–599. [PubMed: 19074988]
- Ducy P, Desbois C, Boyce B, Pinero G, Story B, Dunstan C, Smith E, Bonadio J, Goldstein S, Gundberg C, et al. Increased bone formation in osteocalcin-deficient mice. *Nature.* 1996; 382:448–452. [PubMed: 8684484]
- Engelke JA, Hale JE, Suttie JW, Price PA. Vitamin K-dependent carboxylase: utilization of decarboxylated bone Gla protein and matrix Gla protein as substrates. *Biochim Biophys Acta.* 1991; 1078:31–34. [PubMed: 2049381]
- Ferron M, Hinoi E, Karsenty G, Ducy P. Osteocalcin differentially regulates beta cell and adipocyte gene expression and affects the development of metabolic diseases in wild-type mice. *Proc Natl Acad Sci U S A.* 2008; 105:5266–5270. [PubMed: 18362359]
- Fisher JE, Rogers MJ, Halasy JM, Luckman SP, Hughes DE, Masarachia PJ, Wesolowski G, Russell RG, Rodan GA, Reszka AA. Alendronate mechanism of action: geranylgeraniol, an intermediate in the mevalonate pathway, prevents inhibition of osteoclast formation, bone resorption, and kinase activation in vitro. *Proc Natl Acad Sci U S A.* 1999; 96:133–138. [PubMed: 9874784]
- Flint AJ, Tiganis T, Barford D, Tonks NK. Development of “substrate-trapping” mutants to identify physiological substrates of protein tyrosine phosphatases. *Proc Natl Acad Sci U S A.* 1997; 94:1680–1685. [PubMed: 9050838]
- Fukumoto S, Martin TJ. Bone as an endocrine organ. *Trends Endocrinol Metab.* 2009; 20:230–236. [PubMed: 19546009]
- Hinoi E, Gao N, Jung DY, Yadav V, Yoshizawa T, Myers MG Jr, Chua SC Jr, Kim JK, Kaestner KH, Karsenty G. The sympathetic tone mediates leptin’s inhibition of insulin secretion by modulating osteocalcin bioactivity. *J Cell Biol.* 2008; 183:1235–1242. [PubMed: 19103808]
- Hwang YC, Jeong IK, Ahn KJ, Chung HY. The uncarboxylated form of osteocalcin is associated with improved glucose tolerance and enhanced beta-cell function in middle-aged male subjects. *Diabetes Metab Res Rev.* 2009; 25:768–772. [PubMed: 19877133]
- Kaji H, Hisa I, Inoue Y, Naito J, Sugimoto T, Kasuga M. Analysis of factors affecting increase in bone mineral density at lumbar spine by bisphosphonate treatment in postmenopausal osteoporosis. *J Bone Miner Metab.* 2009; 27:76–82. [PubMed: 19018454]
- Kanazawa I, Yamaguchi T, Yamamoto M, Yamauchi M, Kurioka S, Yano S, Sugimoto T. Serum osteocalcin level is associated with glucose metabolism and atherosclerosis parameters in type 2 diabetes mellitus. *J Clin Endocrinol Metab.* 2009; 94:45–49. [PubMed: 18984661]
- Karsenty G. Convergence between bone and energy homeostases: Leptin regulation of bone mass. *Cell Metab.* 2006; 4:341–348. [PubMed: 17084709]
- Kasuga M, Fujita-Yamaguchi Y, Blithe DL, White MF, Kahn CR. Characterization of the insulin receptor kinase purified from human placental membranes. *J Biol Chem.* 1983; 258:10973–10980. [PubMed: 6309826]
- Konner AC, Janoschek R, Plum L, Jordan SD, Rother E, Ma X, Xu C, Enriori P, Hampel B, Barsh GS, et al. Insulin Action in AgRP-Expressing Neurons Is Required for Suppression of Hepatic Glucose Production. *Cell Metab.* 2007; 5:438–449. [PubMed: 17550779]
- Kulkarni RN, Bruning JC, Winnay JN, Postic C, Magnuson MA, Kahn CR. Tissue-specific knockout of the insulin receptor in pancreatic beta cells creates an insulin secretory defect similar to that in type 2 diabetes. *Cell.* 1999; 96:329–339. [PubMed: 10025399]
- Lee NK, Sowa H, Hinoi E, Ferron M, Ahn JD, Confavreux C, Dacquin R, Mee PJ, McKee MD, Jung DY, et al. Endocrine regulation of energy metabolism by the skeleton. *Cell.* 2007; 130:456–469. [PubMed: 17693256]

- Michael MD, Kulkarni RN, Postic C, Previs SF, Shulman GI, Magnuson MA, Kahn CR. Loss of insulin signaling in hepatocytes leads to severe insulin resistance and progressive hepatic dysfunction. *Mol Cell*. 2000; 6:87–97. [PubMed: 10949030]
- Pittas AG, Harris SS, Eliades M, Stark P, Dawson-Hughes B. Association between serum osteocalcin and markers of metabolic phenotype. *J Clin Endocrinol Metab*. 2009; 94:827–832. [PubMed: 19088165]
- Puigserver P, Rhee J, Donovan J, Walkey CJ, Yoon JC, Oriente F, Kitamura Y, Altomonte J, Dong H, Accili D, et al. Insulin-regulated hepatic gluconeogenesis through FOXO1-PGC-1 α interaction. *Nature*. 2003; 423:550–555. [PubMed: 12754525]
- Rached MT, Kode A, Silva BC, Jung DY, Gray S, Ong H, Paik JH, DePinho RA, Kim JK, Karsenty G, et al. FoxO1 expression in osteoblasts regulates glucose homeostasis through regulation of osteocalcin in mice. *J Clin Invest*. 2010a; 120:357–68. [PubMed: 20038793]
- Rached MT, Kode A, Xu L, Yoshisawa Y, Paik JH, DePinho RA, Kousteni S. FoxO1 is a Positive Regulator of Bone Formation by Favoring Protein Synthesis and Resistance to Oxidative Stress in Osteoblasts. *Cell Metab*. 2010b; 11:147–60. [PubMed: 20142102]
- Sadler JE. Medicine: K is for koagulation. *Nature*. 2004; 427:493–494. [PubMed: 14765176]
- Schaller S, Henriksen K, Sorensen MG, Karsdal MA. The role of chloride channels in osteoclasts: CIC-7 as a target for osteoporosis treatment. *Drug News Perspect*. 2005; 18:489–495. [PubMed: 16391718]
- Scheen AJ. Drug interactions of clinical importance with antihyperglycaemic agents: an update. *Drug Saf*. 2005; 28:601–631. [PubMed: 15963007]
- Schlessinger J. Cell signaling by receptor tyrosine kinases. *Cell*. 2000; 103:211–225. [PubMed: 11057895]
- Scimeca JC, Franchi A, Trojani C, Parrinello H, Grosgeorge J, Robert C, Jaillon O, Poirier C, Gaudray P, Carle GF. The gene encoding the mouse homologue of the human osteoclast-specific 116-kDa V-ATPase subunit bears a deletion in osteosclerotic (oc/oc) mutants. *Bone*. 2000; 26:207–213. [PubMed: 10709991]
- Silver IA, Murrills RJ, Etherington DJ. Microelectrode studies on the acid microenvironment beneath adherent macrophages and osteoclasts. *Exp Cell Res*. 1988; 175:266–276. [PubMed: 3360056]
- Takahashi N, Akatsu T, Udagawa N, Sasaki T, Yamaguchi A, Moseley JM, Martin TJ, Suda T. Osteoblastic cells are involved in osteoclast formation. *Endocrinology*. 1988; 123:2600–2602. [PubMed: 2844518]
- Teitelbaum SL, Ross FP. Genetic regulation of osteoclast development and function. *Nat Rev Genet*. 2003; 4:638–649. [PubMed: 12897775]
- Yamauchi M, Yamaguchi T, Nawata K, Takaoka S, Sugimoto T. Relationships between undercarboxylated osteocalcin and vitamin K intakes, bone turnover, and bone mineral density in healthy women. *Clin Nutr*. 2010 In press.
- Yoshizawa T, Hinoi E, Jung DY, Kajimura D, Ferron M, Seo J, Graff JM, Kim JK, Karsenty G. The transcription factor ATF4 regulates glucose metabolism in mice through its expression in osteoblasts. *J Clin Invest*. 2009; 119:2807–2817. [PubMed: 19726872]

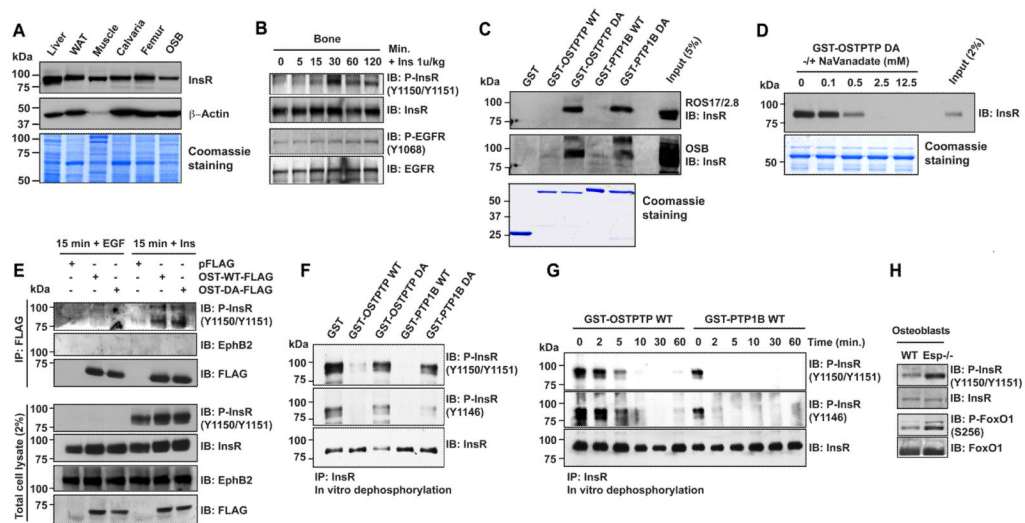


Figure 1. Insulin receptor is a substrate of OST-PTP in osteoblasts

(A) Western blot analysis of insulin receptor (InsR) expression in tissues and primary osteoblasts (OSB).

(B) In vivo phosphorylation of InsR and EGFR in bone following injection of a bolus of insulin.

(C) In vitro substrate trapping. Extracts from pervanadate-treated ROS17/2.8 cells or primary osteoblasts (OSB) were pulled down using GST or WT and DA mutants of OST-PTP and PTP1B GST-fusion proteins. InsR was detected by western blot.

(D) In vitro substrate trapping conducted as described in (C) in absence or presence of increasing concentration of sodium orthovanadate (NaVanadate).

(E) In vivo substrate trapping. OST-PTP-WT and -DA FLAG tagged proteins were immunoprecipitated from ROS17/2.8 cells after 15 minutes stimulation with EGF (100 ng/ml) or insulin (100 nM). Immunoprecipitated proteins (IP) and total cell lysates were then analyzed by western blot.

(F) In vitro dephosphorylation assay. Hyperphosphorylated InsR was immunoprecipitated (IP) from pervanadate-treated ROS17/2.8 extracts, incubated with indicated recombinant proteins for 30 min and visualized by western blot.

(G) Time course of InsR dephosphorylation in vitro by OST-PTP and PTP1B. Experiment was conducted as in (E) except that incubations were stopped at the indicated times.

(H) Phosphorylation of InsR and FoxO1 in unstimulated WT and *Esp*^{-/-} osteoblasts. See also Figure S1.

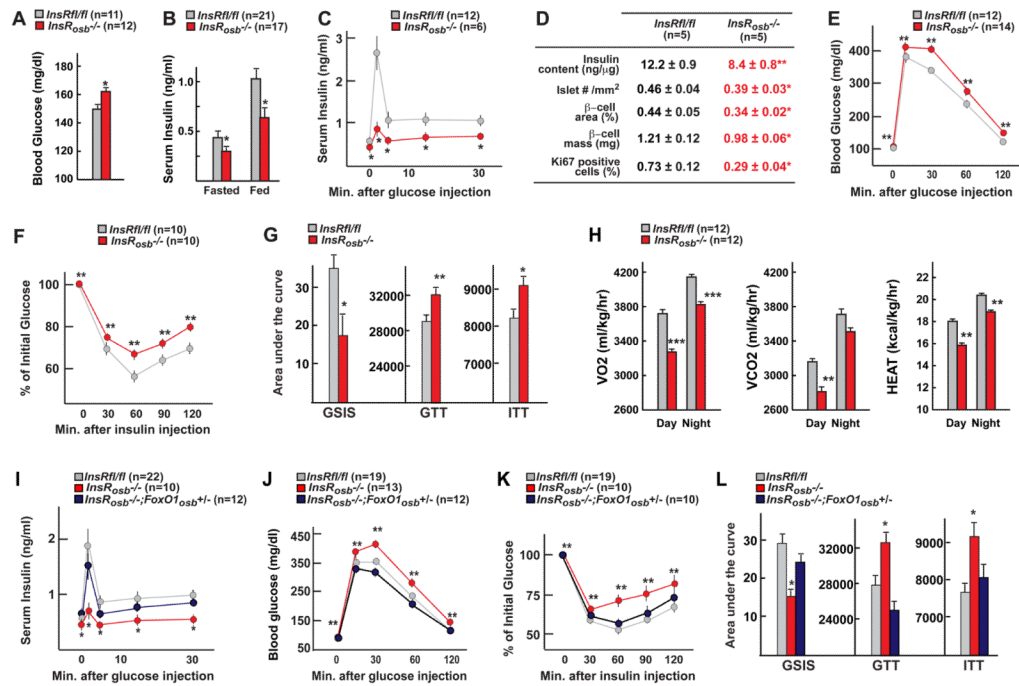


Figure 2. Decreased insulin secretion, glucose tolerance and insulin tolerance in *InsR_{osb}^{-/-}* mice

All experiments compare 8–12 week-old male mice; genotypes are indicated in each panel.

(A) Random fed blood glucose levels.

(B) Fasted and random fed insulin levels.

(C) GSIS.

(D) Pancreas insulin content and histomorphometric comparisons of islet number, islet size, β-cell mass and Ki67 immunoreactive cells in pancreatic islets.

(E) GTT.

(F) ITT.

(G) Area under the curve of C, E and F.

(H) Energy balance data: oxygen consumed (VO₂), carbon dioxide produced (VCO₂) and Heat.

(I–L) Rescue of the *InsR_{osb}^{-/-}* phenotype by *FoxO1* haploinsufficiency, (I) GSIS, (J) GTT, (K) ITT. (L) Area under the curve of I, J and K.

*p<0.05 and **p<0.01 and ***p<0.001 vs *InsRfl/fl* in A–H (t-test or ANOVA) or vs *InsRfl/fl* and *InsR_{osb}^{-/-};FoxO1^{osb+/+}* in I–L (ANOVA).

See also Figure S2.

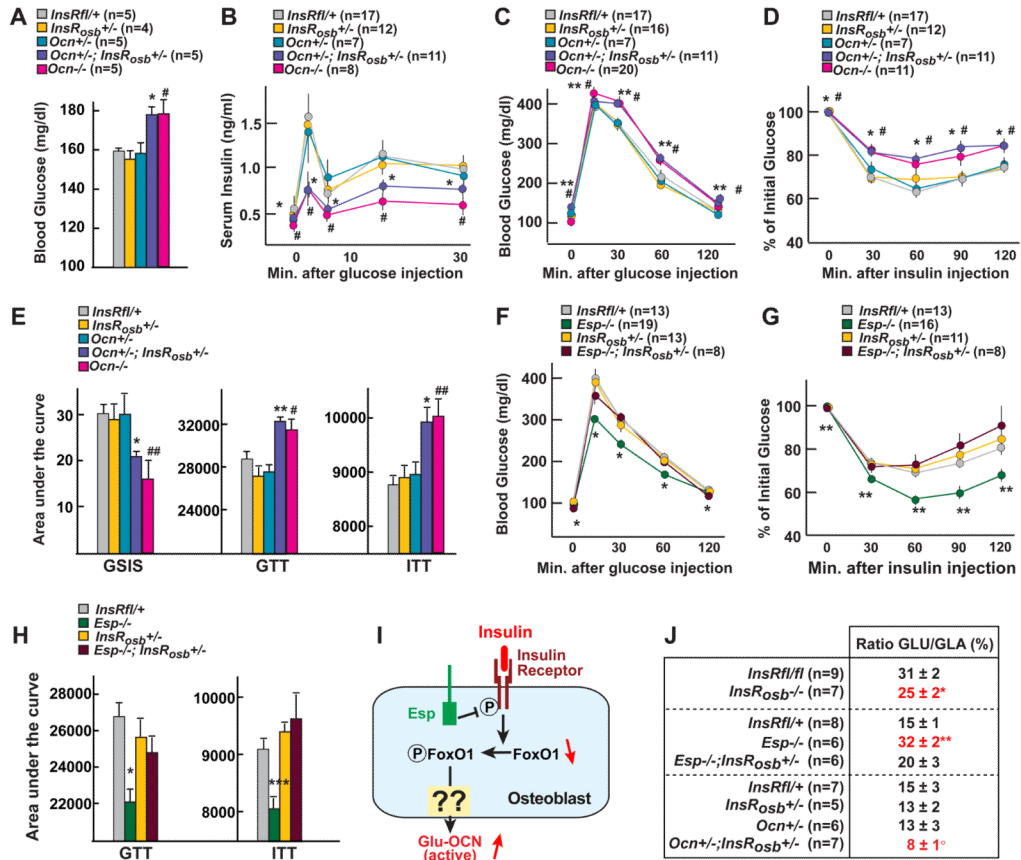


Figure 3. Genetic interaction between *InsR*, *Esp* and *Osteocalcin*

All experiments compare 6–8 week-old male mice unless otherwise noted.

(A) Random fed blood glucose level.

(B) GSIS.

(C and F) GTT.

(D and G) ITT.

(E) Area under the curve of B, C and D.

(H) Area under the curve of F and G.

(I) Model of InsR signaling in osteoblasts.

(J) Carboxylation levels of serum osteocalcin assessed by GLU/GLA dual ELISA.

In (A–E), **p*<0.05 and ***p*<0.01 *InsRosb^{+/-};/Ocn^{+/-}* vs *InsRfl/+*, *InsRosb^{+/-}* and *Ocn^{+/-}* (ANOVA). #*p*<0.05 and ##*p*<0.01 *Ocn^{-/-}* vs *InsRfl/+*, *InsRosb^{+/-}* and *Ocn^{+/-}* (ANOVA).

In (F–H), **p*<0.05, ***p*<0.01 and ****p*<0.001 vs *InsRfl/+*, *InsRosb^{+/-}* and *Esp^{-/-}*; *InsRosb^{+/-}* (ANOVA). In (J), **p*<0.05 vs *InsRfl/fl* (t-test). °*p*<0.05 vs *InsRfl/+* (t test).

See also Figure S3.

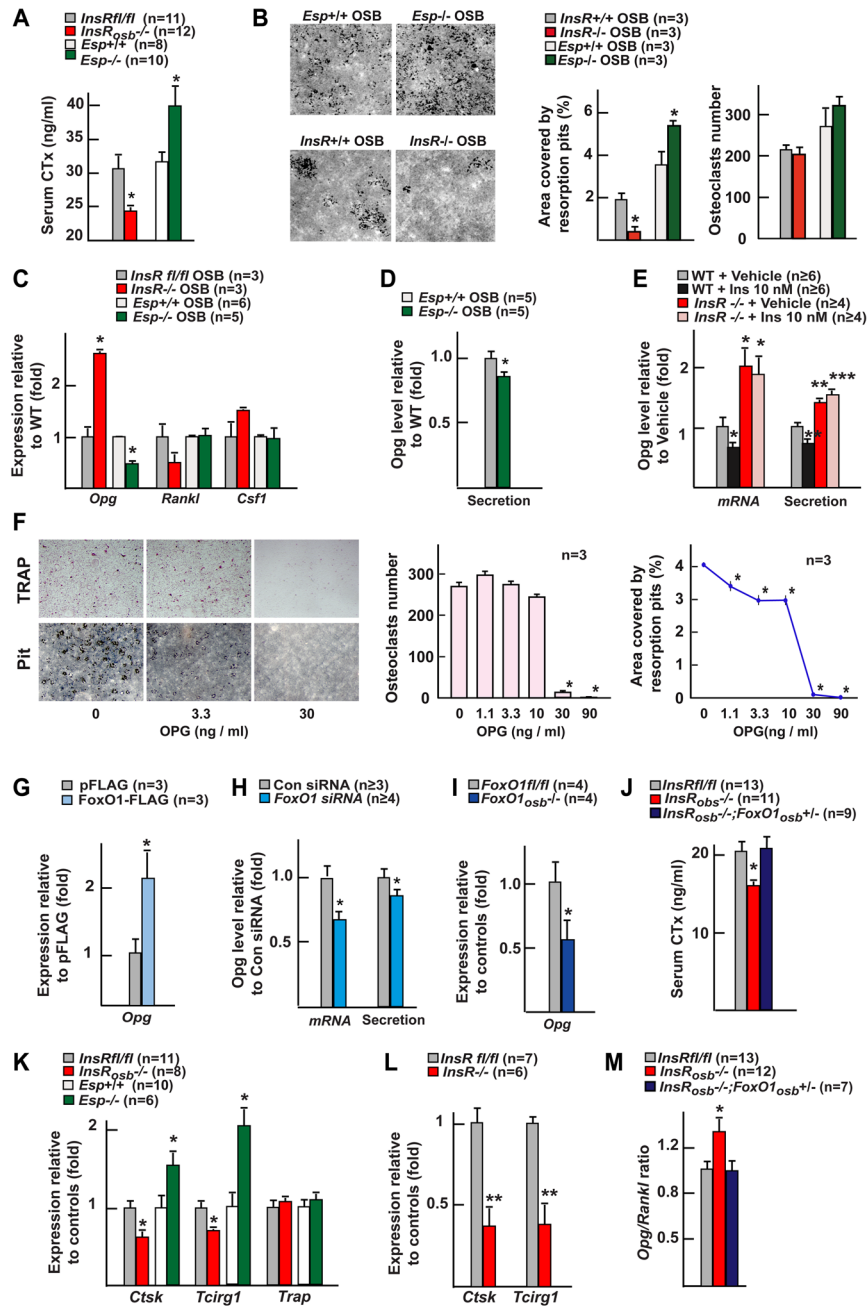


Figure 4. Insulin signaling in osteoblasts favors osteoclast function

Mice genotypes are indicated in each panel.

(A) CTx serum levels in 8 week-old mice.

(B) Differentiation and resorptive ability of osteoclasts co-cultured in presence of control or mutant osteoblasts.

(C) Expression of *Opg*, *Rankl* and *Csf1* in mouse osteoblasts by real-time PCR.

(D) Secretion of OPG in *Esp^{-/-}* and WT osteoblasts.

(E) *Opg* expression and OPG secretion in osteoblasts following a 4h and 24h insulin treatment, respectively.

(F) Dose dependent effects of OPG on differentiation and resorptive ability of osteoclasts in presence of 30ng/ml RANKL and 10 ng/ml M-CSF. Representative pictures of TRAP staining and pit assay (left panel). Quantification of the number of the pits area (middle panel) and of TRAP positive cells (right panel).

(G–H) Real-time PCR analysis of *Opg* expression and/or secretion in ROS17/2.8 osteoblastic cells transfected with empty (pFLAG) or FoxO1 expression (FoxO1-FLAG) vector (G) or in mouse osteoblasts transfected with control siRNA (Con siRNA) or FoxO1 siRNA (H).

(I and J) Expression of *Opg* in bone (I) and CTx serum levels (J) in 1 and 3 month-old mice.

(K, L) Real-time PCR analysis of *Ctsk*, *Tcirg1* and *Trap* expression in bone (K) and in osteoclasts co-cultured in presence of control or *InsR*^{-/-} osteoblasts (L).

(M) Real-time PCR analysis of the *Opg/Rankl* expression ratio in bones of 3 month-old male mice.

In (A–D, G–I, K–L), *p<0.05 and **p<0.01 vs corresponding controls (t-test). In (F), *p<0.05 vs 0ng/ml OPG (t-test). In (E) *p<0.05 vs WT+vehicle (ANOVA). In (J, M) *p<0.05 vs *InsR*^{fl/fl} and *InsRosb*^{-/-}; *FoxO1osb*^{+/-} (ANOVA). See also Figure S4.

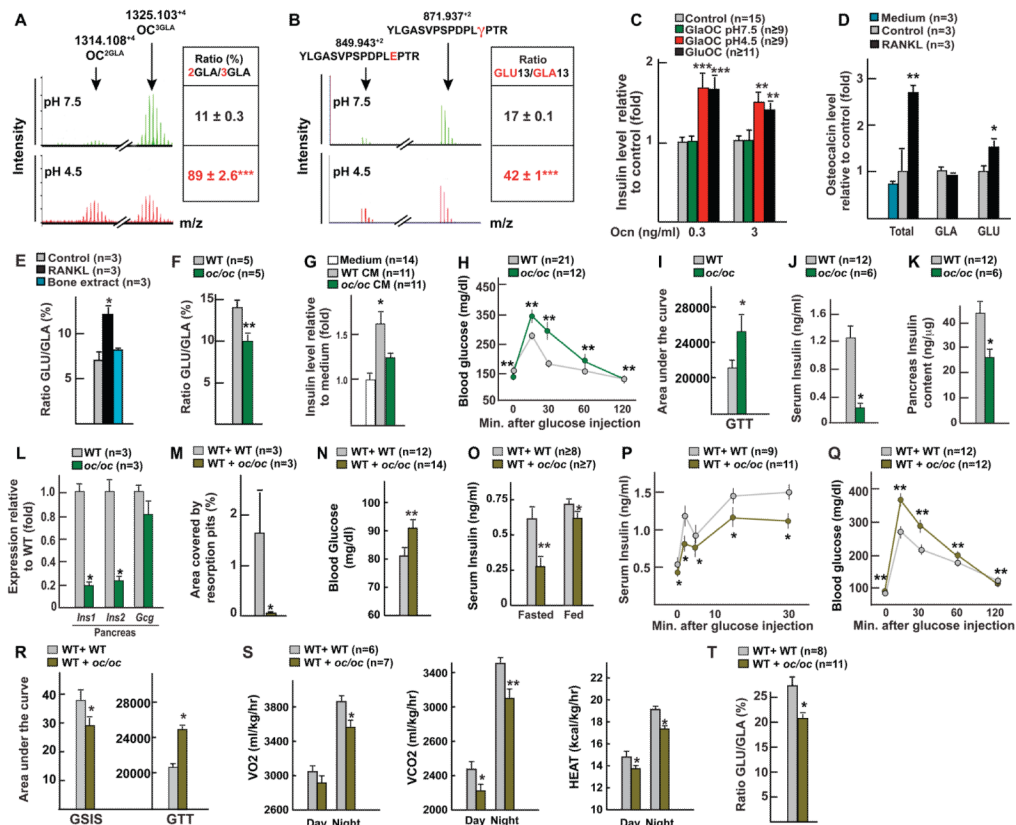


Figure 5. An acidic environment suffices to decarboxylate osteocalcin γ -carboxyglutamic acid 13 (A) High resolution mass spectrometry analysis of carboxylated osteocalcin incubated for 2 weeks at pH7.5 or pH4.5.

(B) Tandem mass spectrometry analysis of trypsin-digested samples of carboxylated osteocalcin incubated at pH 7.5 and 4.5.

(C) Insulin secretion from INS-1 cells following a 1h treatment with the indicated forms of osteocalcin.

(D) Total, GLA and GLU osteocalcin released from bovine bone slices seeded with osteoclast progenitors treated with RANKL or vehicle or medium alone measured by ELISA.

(E) GLU/GLA ratio of the osteocalcin released from bovine bone slices seeded with osteoclast progenitors treated with RANKL or vehicle and osteocalcin chemically extracted from bone slide measured by dual ELISA.

(F–L) Analysis of 2–3 week-old WT and *oc/oc* mice. (F) Carboxylation ratio of serum osteocalcin measured by dual ELISA. (G) Insulin secretion from INS-1 cells following a 1h treatment with conditioned media (CM) from ex-vivo cultures of calvaria from WT and *oc/oc* mice. (H) GTT at 2 weeks of age by IP injecting mice with glucose (1g/kg) under random fed condition. (I) Area under the curve of H. (J) Random fed insulin levels. (K) Pancreas insulin content. (L) Expression of *Insulin* genes (*Ins1* and *Ins2*) and *Glucagon* (*Gcg*) in pancreas by real-time PCR.

(M–T) Analysis of 10–12 week-old WT mice transplanted with either WT (WT+WT) or *oc/oc* (WT+*oc/oc*) fetal liver hematopoietic stem cells. (M) Quantification of the resorptive ability of osteoclasts derived from transplanted mice cultured in presence of RANKL and M-CSF. (N) Random fed blood glucose levels. (O) Fasted and random fed insulin levels. (P) GSIS. (Q) GTT. (R) Area under the curve of P and Q. (S) Energy balance data: oxygen

consumed (VO₂), carbon dioxide produced (VCO₂) and Heat. (T) Carboxylation ratio of serum osteocalcin measured by dual ELISA.

In (C), **p<0.01 and ***p<0.001 vs control and GLA-OCN pH7.5 (ANOVA). In (D–E, G), *p<0.05 and **p<0.01 vs control and/or medium (ANOVA). In (F, I–O, R–T), *p<0.05 and **p<0.01 vs WT (t-test). In (H, P–Q), *p<0.05 and **p<0.01 vs WT (ANOVA).

See also Figure S5.

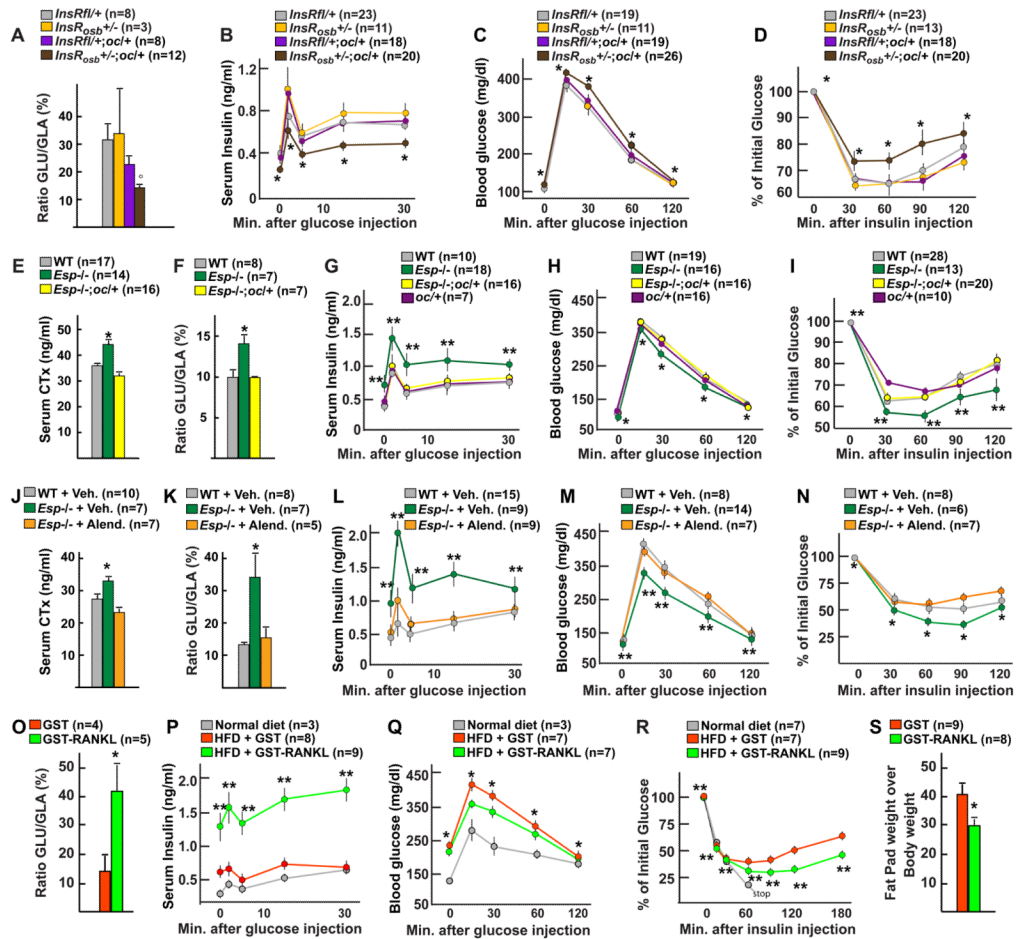


Figure 6. Insulin signaling in osteoblasts favors glucose homeostasis by promoting bone resorption
 (A–I) Analysis of 7–9 week-old (A–D) or 6–7 week-old (D–I) male mice of indicated genotypes.
 (J–N) Analysis of 6 week-old WT and *Esp*^{-/-} mice treated with vehicle (Veh.) or alendronate (Alend., 80µg/kg/week) for 4 weeks.
 (O–S) Analysis of 16 week-old WT mice fed a normal or a high fat diet (HFD) and treated with GST or GST-RANKL (0.8 mg/kg/day) for 8 weeks.
 (A, F, K and O) Carboxylation ratios of serum osteocalcin measured by dual ELISA.
 (B, G, L and P) GSIS.
 (C, H, M and Q) GTT.
 (D, I, N and R) ITT.
 (E, J) CTx serum levels.
 (S) Epididymal fat pad mass.
 In (A), *P <0.05 vs *InsRfl*^{+/+} and *InsRosb*^{+/-} (ANOVA). In (B–D), *p <0.05 vs *InsRfl*^{+/+}, *InsRosb*^{+/-} and *InsRfl*^{+/+};*oc*^{+/+} (ANOVA). In (E–I), *p<0.05 vs WT, *Esp*^{-/-};*oc*^{+/+} and *oc*^{+/+} (ANOVA). In (J–N), *p<0.05 and **p<0.01 vs WT and *Esp*^{-/-} +*Alend* (ANOVA). In (O, S), *p<0.05, **p<0.01 and ***p<0.001 vs GST group (t-test). In (P–R) *p<0.05, **p<0.01 and ***p<0.001 vs Normal diet and GST groups (ANOVA).
 See also Figure S6.

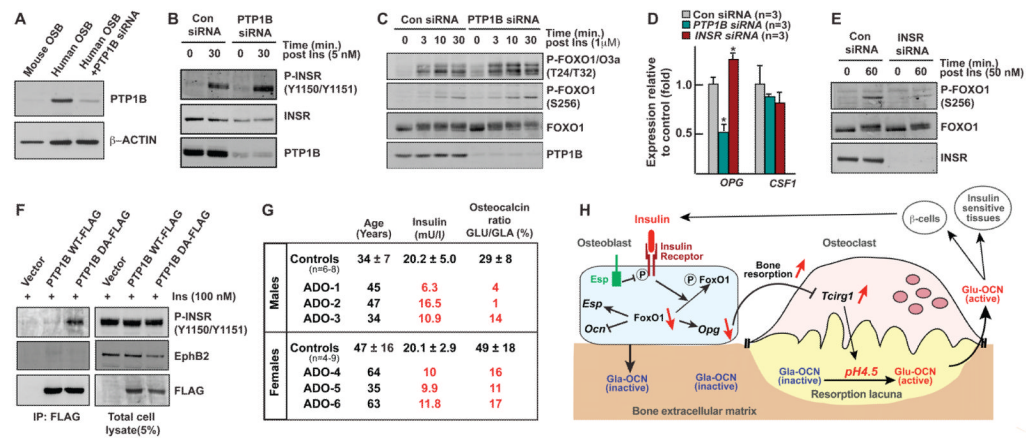


Figure 7. Insulin signaling in human osteoblasts and glucose homeostasis

(A) Western blot analysis of PTP1B expression in human and mouse osteoblasts (OSB).

(B) Phosphorylation of InsR in human osteoblasts transfected with control (Con) or *PTP1B* siRNA.

(C) Phosphorylation of FoxO1 in human osteoblasts transfected with control (Con) or *PTP1B* siRNA.

(D) Real-time PCR analysis of *Opg* expression in human osteoblasts transfected with control siRNA (Con siRNA) or InsR siRNA or *PTP1B* siRNA.

(E) Phosphorylation of FoxO1 in human osteoblasts transfected with control (Con) or *INSR* siRNA.

(F) In vivo trapping of INSR by PTP1B DA mutant in human osteoblasts.

(G) Insulin levels (90 min. post-feeding) and osteocalcin carboxylation ratio assessed by dual ELISA in human patients affected with dominant osteopetrosis (ADO) and normal controls.

(H) Model of the bone resorption-dependent activation of osteocalcin by InsR. Insulin signaling in osteoblasts, which is inhibited by *Esp*, decreases in a FoxO1-dependent manner *Opg* expression. This promotes bone resorption and in particular *Tcigr1* expression and acidification of the bone ECM, which promotes osteocalcin decarboxylation and as a result β -cells proliferation, insulin secretion and insulin sensitivity.

See also Figure S7.